

# Journal of Materials Chemistry C

Accepted Manuscript



This is an *Accepted Manuscript*, which has been through the Royal Society of Chemistry peer review process and has been accepted for publication.

*Accepted Manuscripts* are published online shortly after acceptance, before technical editing, formatting and proof reading. Using this free service, authors can make their results available to the community, in citable form, before we publish the edited article. We will replace this *Accepted Manuscript* with the edited and formatted *Advance Article* as soon as it is available.

You can find more information about *Accepted Manuscripts* in the [Information for Authors](#).

Please note that technical editing may introduce minor changes to the text and/or graphics, which may alter content. The journal's standard [Terms & Conditions](#) and the [Ethical guidelines](#) still apply. In no event shall the Royal Society of Chemistry be held responsible for any errors or omissions in this *Accepted Manuscript* or any consequences arising from the use of any information it contains.

## Soluble Oxide Gate Dielectrics Prepared Using the Self-Combustion Reaction for High-Performance Thin-Film Transistors

Eun Jin Bae,<sup>a</sup> Young Hun Kang,<sup>a</sup> Mijeong Han,<sup>a</sup> Changjin Lee,<sup>\*a,b</sup> and Song Yun Cho<sup>\*a</sup>

<sup>a</sup>*Division of Advanced Materials, Korea Research Institute of Chemical Technology, 141 Gajeong-ro, Yuseong-gu, Deajeon 305-600, Republic of Korea. E-mail: [scho@kriict.re.kr](mailto:scho@kriict.re.kr); Fax: +82 42-860-7200; Tel; +82 42-860-7260*

<sup>b</sup>*Department of Chemical Convergence Materials, Korea University of Science and Technology, 217 Gajeong-ro, Yuseong-gu, Deajeon 305-350, Republic of Korea*

†Electronic supplementary information (ESI) available: Transfer and output characteristics with various GPTMS ratios and different composition ratios, dielectric properties, XPS spectra of AlO<sub>x</sub> thin films, TEM cross sectional images, TG-DTA curves of AlO<sub>x</sub> precursors with different composition ratios, and XRD patterns are available. Fig. S1-S8.

We report the fabrication of high-performance metal oxide thin-film transistors (TFTs) with  $\text{AlO}_x$  gate dielectrics using combustion chemistry in a solution process to provide energy to convert oxide precursors into oxides at low temperatures. Our self-combustion system utilizing two Al precursors as a fuel and oxidizer is systematically compared with conventional combustive Al precursors with urea in terms of combustion efficiency and dielectric properties.  $\text{AlO}_x$  gate dielectric layers are spin-coated from a solution of combustive  $\text{AlO}_x$  precursors in 2-methoxyethanol and annealed at 250 °C. In this process, organic compounds can be introduced to improve the resulting layer morphology. The thermal behaviors of the self-combustive  $\text{AlO}_x$  precursors are investigated and compared with those of noncombustive  $\text{AlO}_x$  precursors and combustive urea- $\text{AlO}_x$  precursors to evaluate the generation of exothermic heat at a relatively low annealing temperature. The  $\text{AlO}_x$  dielectrics prepared from self-combustive precursors have uniform and smooth surfaces, low leakage current densities, and high dielectric constants above 8.7. They also exhibit excellent insulating properties and no breakdown at high electric fields. Furthermore, the ZnO TFTs prepared to confirm the operation of the  $\text{AlO}_x$  gate dielectrics show a good mobility of  $24.7 \text{ cm}^2 \text{ V}^{-1} \text{ s}^{-2}$  and an on/off ratio of  $10^5$ . It is believed that the  $\text{AlO}_x$  dielectrics prepared using the self-combustion reaction at low temperature can form a good interface facilitating the growth of desirable ZnO crystal structures, which leads to a considerable improvement in ZnO TFT performance.

## 1. Introduction

The gate dielectric is a critical element affecting the electrical performance of thin-film transistors (TFTs). To obtain high-performance gate dielectrics for TFTs that can provide high capacitance without relying on ultrathin film thicknesses, high- $k$  dielectric materials have been actively pursued to replace SiO<sub>2</sub> (dielectric constant  $\sim 3.9$ ). The high capacitance and thicker layer also allow for efficient charge injection into the transistor channels and reduce the direct-tunneling leakage currents. Such advantages have motivated intense research into the development of zirconium oxide (ZrO<sub>2</sub>), hafnium oxide (HfO<sub>2</sub>), and aluminum oxide (AlO<sub>3</sub>) as high- $k$  dielectric materials.<sup>1-3</sup> However, gate dielectric layers made of these materials must still be fabricated using vacuum processes, which have high costs for processing equipment and facilities.

Recently, numerous research studies into solution-processed TFTs have focused on the development of soluble high- $k$  gate dielectric materials for high-performance TFTs.<sup>4-10</sup> Solution-processability can lead to several advantages including printability, the possibility of large-area deposition, low-cost device fabrication, and compatibility with mechanically flexible substrates.<sup>11-14</sup> Among many potential materials, Al<sub>2</sub>O<sub>3</sub> thin films are well known as high- $k$  gate dielectrics because of their low interfacial trap density with oxide semiconductors and relative permittivity of  $\sim 9$ .<sup>15</sup> For example, a sodium  $\beta$ -alumina gate dielectric prepared using a sol-gel reaction at 830 °C to produce an oxide TFT showed a mobility of 28 cm<sup>2</sup> V<sup>-1</sup> s<sup>-1</sup>.<sup>16</sup> Furthermore, an AlO<sub>x</sub> gate dielectric deposited using a multiple-spin-coating procedure and annealed at 300 °C had an oxide TFT mobility of 33 cm<sup>2</sup> V<sup>-1</sup> s<sup>-1</sup>.<sup>17</sup> Despite these high reported mobilities for oxide TFTs, however, the high processing temperature and multiple spin-coating processes lead to certain limitations.

As an alternative, the solution combustion reaction is an easy and time-saving production process based on thermochemical concepts used in the propellant and explosive fields. Recently, combustion chemistry has been utilized for the synthesis of nanooxides for electronic applications. The advantages of this process derive from the fact that no special equipment is required to provide additional heat, because the combustion reaction of simple precursor compounds itself generates heat that can be used to form the metal oxide.<sup>18,19</sup>

Research into combustion reactions for TFT fabrication has mostly been conducted using metal oxides such as  $\text{In}_2\text{O}_3$ , ZTO, IZO, and ITO.<sup>20,21</sup> However, quite recently the addition of urea as a fuel for combustion to form gate dielectric materials has been introduced.<sup>22</sup> Currently, this approach has several limitations that should be solved, such as a low combustion efficiency and the resulting high leakage current of the resulting dielectric. In particular, the low combustion efficiency can result in insufficient heat supply to the internal system, which leads to unsatisfactory dielectric properties. Moreover, it is quite difficult to finely tune the amount of urea needed to realize the optimal combustion reaction.

Here, we suggest a promising and novel method of synthesizing solution-processable gate dielectrics by self-combustion at low temperatures. Our facile, efficient *self-combustion* process overcomes the shortcomings of previous combustive approaches by simply mixing two metal precursors that contain coordinated fuel and oxidizer ligands. We believe that this simple process can provide more stable TFTs and better dielectric performance because of its high combustive efficiency. In addition, hybridization of the dielectric material with organic polymers can be achieved by carrying out a sol-gel reaction with the  $\text{AlO}_x$  precursors to provide more electrically stable and fine-tuned properties in a high- $k$  gate dielectric layer. In the basic synthesis, the  $\text{AlO}_x$  gate dielectrics for oxide TFTs were obtained by solution combustion from a mixture of  $\text{AlO}_x$

and organic precursors at a low temperature of 250 °C. To confirm the dielectric properties of the  $\text{AlO}_x$  prepared using this combustion system with organic components for use in oxide TFTs, ZnO TFTs were fabricated by spin-coating ZnO precursors on the  $\text{AlO}_x$  films and annealing at 250 °C. Moreover, the crystalline structures of the ZnO on the  $\text{AlO}_x$  films prepared from combusive precursors were compared with those on films prepared from noncombustive precursors and combusive precursors with urea to investigate the influence of the gate dielectric layer on the TFT performance.

## 2. Results and discussion

The combustion reaction between organic fuels (e.g., acetylacetone, urea, carbohydrazide, and citric acid) and an oxidizer (e.g., nitrate) can lower the effective annealing temperature required for the formation of metal oxide compounds from oxide precursors. When a fuel-oxidizer pair is moderately heated, a highly intense exothermic reaction occurs. The evolved heat can accelerate the formation of metal hydroxides or alkoxides into the corresponding metal oxide frameworks (M-O-M) at sufficiently low external temperatures. In other words, in the self-combustion system, the energy required for complete conversion of the precursors into oxides can be replenished by the exothermic energy from the combusive precursor reaction. Previous studies have demonstrated that metal nitrates (as both a metal source and oxidizer) and acetylacetone (AcAc, as both a chelating agent and fuel) are the most effective among the various oxidizers and fuels for self-combustion.<sup>23,24</sup>

To investigate the thermal behavior of the  $\text{AlO}_x$  precursor during the self-combustion reaction, thermogravimetric differential thermal analysis (TG-DTA) was conducted. To compare the thermal properties of combusive precursors with those of noncombustive precursors, TG-DTA

data were plotted for self-combustive  $\text{AlO}_x$  precursors, the  $\text{Al}(\text{NO}_3)_3 \cdot 9\text{H}_2\text{O}$  and  $\text{Al}(\text{C}_2\text{H}_5\text{O}_2)_3$  pair, and the noncombustive precursors  $\text{Al}(\text{NO}_3)_3 \cdot 9\text{H}_2\text{O}$  and  $\text{Al}(\text{C}_2\text{H}_5\text{O}_2)_3$  (Fig. 1). Furthermore, to analyze and compare the thermal behavior of conventional combustive system, a combustive precursor composed of  $\text{Al}(\text{NO}_3)_3 \cdot 9\text{H}_2\text{O}$  and urea as an external fuel was investigated. The DTA data for the self-combustive  $\text{AlO}_x$  precursor containing acetylacetonate (fuel) and nitrate (oxidizer) ligands show a single, intense exothermic peak at 170 °C in Fig. 1(a) that corresponds exactly to the abrupt mass loss. On the other hand, the combustive precursor with urea shows a negligible exothermic peak and no mass loss at around 250 °C, and the combustion efficiency is remarkably lower and the exothermic temperature is much higher than those of the self-combustive precursor. This means that quite a small amount of heat can lead to M-O-M formation in the urea-based combustion system. In the case of the noncombustive the  $\text{Al}(\text{NO}_3)_3 \cdot 9\text{H}_2\text{O}$  precursor, a gradual mass loss is completed at around 400 °C without any exothermic peaks, which is possibly due to the decomposition of organic ligands. Even though the TGA data for the  $\text{Al}(\text{C}_2\text{H}_5\text{O}_2)_3$  precursors show abrupt thermal decomposition at a relatively low temperature of 250 °C, Fig. 2(d) shows that they do not undergo an exothermic reaction. This also implies that the  $\text{Al}(\text{C}_2\text{H}_5\text{O}_2)_3$  precursor is a good candidate for producing  $\text{AlO}_x$  gate dielectrics. However, when the  $\text{AlO}_x$  gate dielectric for a ZnO TFT is prepared using  $\text{Al}(\text{C}_2\text{H}_5\text{O}_2)_3$  precursors at 250 °C, the electrical performance of the resulting ZnO TFT is particularly poor, as shown in Supplementary Information Fig. S1<sup>†</sup>. This means that noncombustive  $\text{AlO}_x$  precursors require a high temperature of over 400 °C for the complete conversion of the precursors into the M-O-M lattice. In addition, this result supports the conclusion that the exothermic heat from a self-combustive  $\text{AlO}_x$  precursor can assist the conversion into the corresponding oxides at low temperatures.

When only the  $\text{AlO}_x$  precursor was deposited without any organic ingredients, the obtained  $\text{AlO}_x$  gate dielectric layer showed a quite poor surface morphology (Fig. 2): the surface of the film was cracked and had numerous pores generated during annealing. The combusive  $\text{AlO}_x$  precursor with urea but no other organic components also shows an improper surface morphology for gate dielectric layer. These poor surface properties can render the  $\text{AlO}_x$  gate dielectric layers prepared from only the  $\text{AlO}_x$  precursor difficult to use in actual devices because of their high leakage currents and because they exhibit charge-trapping phenomena. To improve the layer morphology, organic components such as (3-glycidoxypropyl)trimethoxysilane (GPTMS) can be introduced into the oxide network as polymeric binders using the sol-gel method. To fabricate a stable gate dielectric layer with a smooth surface, the combusive  $\text{AlO}_x$  precursor can be mixed with GPTMS, the epoxy moiety of which polymerizes during the annealing process (Scheme 1).

The dielectric characteristics of the self-combustive  $\text{AlO}_x$  dielectric films and their dependence on the organic content (GPTMS) were evaluated by measuring the quantitative leakage current and dielectric constant. The supplementary information Fig. S2<sup>†</sup> shows typical current density vs. electrical field and capacitance vs. frequency curves for metal-insulator-metal (MIM) structures fabricated from  $\text{AlO}_x$  insulators with various amounts of GPTMS. The plot demonstrates that GPTMS-only films exhibit the highest dielectric constant, and higher GPTMS contents result in higher dielectric constants of the  $\text{AlO}_x$  insulators in the range of 8.7–12. Even though the GPTMS film shows a high dielectric constant of 16 at 100 Hz, this film is unsuitable as a gate dielectric because of its unstable nature in all frequency ranges. Furthermore, GPTMS-only films have high leakage current densities because of their nonuniform and rough surface morphologies. This result means that the dense network structure produced by the sol-gel



reaction of GPTMS together with the hybridization of the  $\text{AlO}_x$  precursors is necessary to obtain a satisfactory surface structure for the final gate dielectric film. When the ratio of the  $\text{AlO}_x$  precursor to GPTMS is 1:8, the dielectric constant of the  $\text{AlO}_x$  films is stable in all frequency ranges. When the ratio of the  $\text{AlO}_x$  precursor to GPTMS decreases to 1:30 or 1:45, the dielectric properties of the obtained films are unstable, especially in the low and high frequency ranges. Consequently, the operating zone of TFTs fabricated with these GPTMS ratios is limited to specific frequency ranges. The dielectric constants of  $\text{AlO}_x$  insulators prepared without GPTMS could not be measured because of film cracking. Therefore, the ratio between the  $\text{AlO}_x$  precursor and GPTMS was chosen to be 1:8 to obtain the optimal TFT characteristics. The leakage current densities for films with thicknesses of  $d = 200$  nm prepared from  $\text{AlO}_x$  precursors with GPTMS with are around  $10^{-8}$ – $10^{-9}$   $\text{A cm}^{-2}$  up to  $E \approx 2$   $\text{MV cm}^{-1}$ . In particular,  $\text{AlO}_x$  insulators prepared with a 1:8 ratio of the  $\text{AlO}_x$  precursor to GPTMS show excellent leakage current densities of  $3.92 \times 10^{-9}$   $\text{A cm}^{-2}$ . All the electrical properties obtained with different  $\text{AlO}_x$  precursor:GPTMS ratios are summarized in Table 1. The excellent insulating properties of the films obtained from combusive  $\text{AlO}_x$  precursors hybridized with an organic component are superior to those of the commonly used solution-processable high- $k$  gate dielectric materials. For the comparison with the conventional combusive precursor,  $\text{AlO}_x$  insulators were prepared by combustion with urea using a 1:8 ratio of the combusive precursor to GPTMS with annealing at 250 °C. Figure 3 shows typical current density vs. electric field and capacitance vs. frequency curves from the GPTMS-containing  $\text{AlO}_x$  films formed by self-combustion and combustion with urea, respectively. The dielectric constant of the  $\text{AlO}_x$  insulators formed by combustion with urea is around 4.4, which is much lower than that of the  $\text{AlO}_x$  formed by self-combustion. In addition, the layer formed by combustion with urea shows a poor leakage current density of  $2.80 \times 10^{-6}$  A

$\text{cm}^{-2}$ , which results from the sparse  $\text{AlO}_x$  lattice structure. We believe that this structural defect originates from the formation of a flimsy M-O-M structure because not enough exothermic heat was supplied to the system owing to the low combustion efficiency of the combustive precursor with urea (Supplementary Information Fig. S3<sup>†</sup>).

To demonstrate the feasibility of the combustive  $\text{AlO}_x$  precursor for forming a gate dielectric layer, ZnO TFTs with a bottom-gate top-contact structure were fabricated from spin-coated ZnO semiconductors on  $\text{AlO}_x$  gate dielectrics that were annealed at 250 °C in air. Al source-drain electrodes of 100 nm thickness were subsequently deposited on the ZnO channel layers. The electrical characteristics of the  $\text{AlO}_x$ -based TFTs with semiconducting ZnO active layers were investigated. The thickness of ZnO channel layer was determined to be approximately 10 nm from cross-sectional transmission electron microscope (TEM) images of the ZnO TFT (Supplementary Information Fig. S4<sup>†</sup>). To realize high field effect mobilities and high on/off current ratios from ZnO TFTs with  $\text{AlO}_x$  gate dielectrics, an equivalent amount of fuel and oxidizer is necessary (Supplementary Information Fig. S5<sup>†</sup> and S6<sup>†</sup>). When the content of fuel is higher than that of oxidizer or *vice versa*, the combustion process may not proceed to completion, resulting in a reduced M-O-M and an increased M-OH composition. Therefore, the  $\text{AlO}_x$  thin films' chemical composition between oxidizer and fuel for the proper electrical performance of the corresponding TFTs was determined to be 1:1. Fig. 4 shows the output and transfer curves of ZnO TFTs with  $\text{AlO}_x$  gate dielectric layers prepared with a 1:8 ratio of the combustive  $\text{AlO}_x$  precursor to GPTMS. The field-effect mobility of ZnO TFTs with  $\text{AlO}_x$  gate dielectrics prepared from combustive precursors with urea is  $2.48 \times 10^{-3} \text{ cm}^2 \text{ V}^{-1} \text{ s}^{-1}$ , and their on/off ratio of  $10^4$ , with a large hysteresis. Such poor electric performance of ZnO TFTs with  $\text{AlO}_x$  gate dielectrics prepared by combustion with urea can be attributed to insufficient dielectric properties of the

gate dielectric layer due to the low combustion efficiency of the precursors. In contrast, ZnO TFTs with AlO<sub>x</sub> gate dielectrics prepared from self-combustive precursors exhibit an improved field-effect mobility of 24.7 cm<sup>2</sup> V<sup>-1</sup> s<sup>-1</sup> and an on/off ratio of 10<sup>5</sup>. Furthermore, these ZnO TFTs show good operating stability and excellent mobility with good switching characteristics. The output curve of this ZnO TFT has clear pitch-off characteristics and good current saturation.

In addition, we investigated the device uniformity, which is of substantial importance for practical use of TFTs. To measure the uniformity of ZnO TFTs, 20 TFT units were fabricated with 1:8 ratios of the self-combustive AlO<sub>x</sub> precursor to GPTMS using an annealing temperature of 250 °C. The performance of the TFT units was measured, and standard deviations were obtained for the mobility ( $\mu = 23.1 \pm 5.22 \text{ cm}^2 \text{ V}^{-1} \text{ s}^{-1}$ ) and turn-on voltage ( $V_{\text{on}} = 7.87 \pm 3.4 \text{ V}$ ) (Fig. 4(e)). It was found that the ZnO TFTs with AlO<sub>x</sub> gate dielectrics prepared by self-combustion exhibit good device uniformity and reproducible yields. The mobility, threshold voltage, and on/off ratio are summarized in Table 2. The mobility values for different self-combustive AlO<sub>x</sub> precursor/GPTMS ratios are in the range of 8.97–24.7 cm<sup>2</sup> V<sup>-1</sup> s<sup>-1</sup>, as calculated by extrapolating the capacitance values to a frequency of 1 Hz.<sup>16</sup> Although the ZnO TFTs with other self-combustive AlO<sub>x</sub> precursor/GPTMS ratios operated properly, their output characteristics are unstable, as shown in Supplementary Information Fig. S7<sup>†</sup>.

To further investigate the nanocrystalline structures of the AlO<sub>x</sub> gate dielectrics prepared from combustive precursors, TEM analysis was performed. As shown in Fig. 5, no AlO<sub>x</sub> nanocrystallites were present in films prepared by either combustion with urea or without combustion. However, the AlO<sub>x</sub> nanocrystallites were uniformly embedded in the AlO<sub>x</sub> gate dielectric layer prepared by self-combustion. All of the nanocrystallites possess a lattice structure, as shown in the TEM image in Fig. 5(a) (inset). We believe that the strong combustion

reaction of the self-combustive precursor provides sufficient external heat to generate  $\text{AlO}_x$  nanocrystallites, whereas the weak or absent combustion reactions of the other precursors do not generate enough energy to form crystal structures. The existence of the  $\text{AlO}_x$  nanocrystalline lattice further proves that the bottom  $\text{AlO}_x$  structure facilitates the vertical crystal growth of ZnO crystals when the self-combustive  $\text{AlO}_x$  precursors are used. The crystal lattice mismatch between ZnO and  $\text{AlO}_x$  is reduced by the existence of nanocrystalline  $\text{AlO}_x$  beneath the ZnO layer, so this environment is more favorable for the vertical ZnO crystal growth. The surface morphology of the ZnO films grown on the  $\text{AlO}_x$  films was analyzed using an atomic force microscope (AFM). Figure 6 shows the surface characteristics of the  $\text{AlO}_x$  films with and without GPTMS prepared by self-combustion. The roughness of the gate dielectric affects the surface morphology of the channel layer in the bottom-gate TFTs. The root mean square (RMS) roughness value of the ZnO film on the  $\text{AlO}_x$  film with GPTMS is 1.19 nm, which means that the surface is much denser and smoother than that of the ZnO film without GPTMS, which has an RMS roughness of 10.4 nm. The improved surface morphology of the ZnO films proves that there is a synergetic function of the  $\text{AlO}_x$  gate dielectric with GPTMS that enhances the carrier mobility and overall performance of ZnO TFTs.

To investigate the possible reason for the significantly enhanced field-effect mobility of ZnO TFTs containing  $\text{AlO}_x$  gate dielectrics produced from self-combustive precursors at low annealing temperatures, the crystallinity of the ZnO deposited on the obtained  $\text{AlO}_x$  layer was analyzed using the thin-film diffraction method (Fig. 7). For comparison,  $\text{AlO}_x$  gate dielectrics were prepared from combustive and noncombustive  $\text{Al}(\text{C}_2\text{H}_5\text{O}_2)_3$  and  $\text{Al}(\text{NO}_3)_3 \cdot 9\text{H}_2\text{O}$  precursors with GPTMS ratios of 1:8 at 250 °C, respectively. The ZnO films with  $\text{AlO}_x$  gate dielectrics prepared using these combustive and noncombustive precursors show amorphous-like diffraction

patterns with no significant diffraction peaks, whereas relatively strong polycrystalline peaks of ZnO are clearly apparent in the ZnO films on AlO<sub>x</sub> gate dielectrics prepared from self-combustive precursors. Interestingly, the intensity of the (002) peak is relatively stronger than that of the (100) and (101) peaks in the ZnO film prepared on the AlO<sub>x</sub> gate dielectric prepared from the self-combustive precursor, indicating that the direction of the ZnO crystals is preferentially with the *c*-axis oriented along the surface of the AlO<sub>x</sub> gate dielectric. The preferential orientation of the (002) direction indicates vertical growth of the ZnO crystals, which is advantageous for the enhancement the TFT mobility because it provides a favorable charge conduction pathway. It is believed that the more crystalline nature of the AlO<sub>x</sub> layer due to the additional heat supplied by the self-combustive precursors can affect the microstructure of the adjacent ZnO layer (Supplementary Information Fig. S8<sup>†</sup>), as compared to the case for the layers produced from the combustive precursor with urea or the noncombustive precursor. During the annealing of the ZnO layer, the more crystalline structure of the AlO<sub>x</sub> prepared from self-combustive precursors beneath the ZnO layer can reduce the amount of interruption of the crystal formation due to lattice mismatching, which ultimately leads to the more crystalline character of the grown ZnO.<sup>25-28</sup> Consequently, the self-combustion reaction of the AlO<sub>x</sub> precursors results in a more crystalline structure of the final AlO<sub>x</sub> dielectric annealed at a low temperature, which yields a favorable semiconducting ZnO crystal structure for good TFT characteristics.

### 3. Conclusions

We successfully fabricated an AlO<sub>x</sub> gate dielectric using a self-combustion reaction in a solution process at a low temperature of 250 °C. The self-combustion of the AlO<sub>x</sub> precursors was investigated in terms of their thermal behaviors, and the combustive AlO<sub>x</sub> precursors were

converted into high- $k$   $\text{AlO}_x$  gate dielectrics at low temperatures by the self-combustion reaction. In addition, organic components (GPTMS) were incorporated into the soluble  $\text{AlO}_x$  precursors using the sol-gel method to improve the surface properties, which can provide a well-defined interface between the gate dielectric and the active layer. The electrical characteristics of the  $\text{AlO}_x$  gate dielectrics with various amounts of GPTMS were analyzed and compared. The dielectric constants and capacitances of  $\text{AlO}_x$  gate dielectrics with  $\text{AlO}_x$  precursor:GPTMS ratios higher than 1:8 are unstable in the low- and high-frequency ranges. The  $\text{AlO}_x$  gate dielectric layer prepared using a 1:8 ratio of combustive  $\text{AlO}_x$  precursor to GPTMS exhibits quite stable insulating properties with a leakage current density of  $1.80 \times 10^{-8} \text{ A cm}^{-2}$ . Furthermore, the  $\text{AlO}_x$  dielectrics prepared from self-combustive precursors exhibit a high dielectric constant of 8.7. In comparison, the layer prepared from the combustive  $\text{AlO}_x$  precursor composed of  $\text{Al}(\text{NO}_3)_3 \cdot 9\text{H}_2\text{O}$  and urea as an additional fuel, which has been studied previously, shows quite unsatisfactory dielectric properties and a high leakage current due to the low combustion efficiency. The ZnO TFTs with high- $k$   $\text{AlO}_x$  prepared from self-combustive precursors show an excellent field-effect mobility of  $24.7 \text{ cm}^2 \text{ V}^{-1} \text{ s}^{-1}$  and an on/off ratio of  $10^5$ . Such significant enhancement of the mobility of ZnO TFTs due to the vertical growth of the ZnO crystal structure can be attributed to the crystalline structure of the  $\text{AlO}_x$  gate dielectric prepared from the combustive precursors beneath the ZnO layer. This crystallinity was promoted by the heat provided by the combustion reaction. Hence, these electrically stable  $\text{AlO}_x$  gate dielectrics prepared using low-temperature processing demonstrate the potential application of the proposed system in the field of flexible printed electronics.

#### 4. Experimental section

## Instrumentation

A TG-DTA (SDT 2060, TA Instruments, USA) was used to measure the thermal behaviors of the  $\text{AlO}_x$  precursors, which were dried at  $70\text{ }^\circ\text{C}$  for 24 h. Samples of about 10 mg to 15 mg were heated from room temperature to  $700\text{ }^\circ\text{C}$  at a heating rate of  $10\text{ }^\circ\text{C}/\text{min}$  in ambient air in all cases. An X-ray diffractometer (XRD; RIGAKU Co., Japan) was used to identify the crystal structures of the ZnO thin films coated on the  $\text{AlO}_x$  gate dielectrics and  $\text{AlO}_x$  thin films. XRD measurements were performed using the thin film diffraction technique, in which samples were fixed at low angle of  $3^\circ$  to the X-ray beam during the  $2\theta$  scan of the detector. The source power was 60 mA/40 kV, which is stronger than the power used in normal XRD. To investigate the nanocrystalline structure of the  $\text{AlO}_x$  film, TEM (JEOL Ltd., Japan) was employed. The TEM samples were prepared by spin-coating the  $\text{AlO}_x$  precursor onto a copper grid. The prebaking and annealing process were conducted in the same manner used for MIM device fabrication described below. The cross sections of the ZnO TFTs were also investigated by TEM. The cross-sectional samples were cut by a focused ion beam (JEOL Ltd., Japan). The surface morphology of the  $\text{AlO}_x$  films and ZnO thin films were investigated using a SEM (Philips XL30S FEG, Netherlands) and AFM (Nanoscope System Co., Korea) in an area of  $3\text{ }\mu\text{m}^2$  in noncontact mode. Before the analysis of the films, platinum films with a thickness of approximately 100 nm were deposited on the prepared films with a coating machine (E-1030, Hitachi Ltd., Japan).

## Preparation of self-combustive and noncombustive $\text{AlO}_x$ precursor solutions

For the combustive  $\text{AlO}_x$  precursor solutions, aluminum nitrate nonahydrate ( $\text{Al}(\text{NO}_3)_3 \cdot 9\text{H}_2\text{O}$ , 99.997%) and aluminum acetylacetonate ( $\text{Al}(\text{C}_2\text{H}_5\text{O}_2)_3$ , 99%) were dissolved in anhydrous 2-methoxyethanol. All chemicals for this procedure were obtained from Sigma-Aldrich. The

noncombustive  $\text{AlO}_x$  precursor solutions were prepared with equivalent concentrations of 0.05 M  $\text{Al}(\text{NO}_3)_3 \cdot 9\text{H}_2\text{O}$  and 0.05 M  $\text{Al}(\text{C}_2\text{H}_5\text{O}_2)_3$  in 10 ml of anhydrous 2-methoxyethanol. The solutions were thoroughly stirred for more than 2 h at room temperature to prepare the homogeneous precursor solution. The total concentration of  $\text{AlO}_x$  precursor solution was fixed at 1 M. To improve the surface properties of the  $\text{AlO}_x$  films, GPTMS solutions were added into the  $\text{AlO}_x$  precursor solutions in various molar ratios. The GPTMS solutions were prepared by hydrolyzing GPTMS in 2-propanol by adding a dilute aqueous solution of  $\text{HNO}_3$  and stirring at room temperature for 1 h.<sup>29</sup> For the comparison of self-combustive  $\text{AlO}_x$  precursor solutions with noncombustive precursors for  $\text{AlO}_x$  gate dielectrics, two types were prepared by separately dissolving 1 M  $\text{Al}(\text{NO}_3)_3 \cdot 9\text{H}_2\text{O}$  and 1 M  $\text{Al}(\text{C}_2\text{H}_5\text{O}_2)_3$  in 10 ml of anhydrous 2-methoxyethanol.

#### **Preparation of urea-combustive $\text{AlO}_x$ precursor solutions**

The combustive precursor solutions with urea were prepared as described in the literature.<sup>22</sup>

#### **Preparation of ZnO precursor solutions**

For the ZnO precursors, 0.1 M zinc hydroxide ( $\text{Zn}(\text{OH})_2$ , 98%, Junsei Co., Japan) was dissolved in 10 ml of ammonium hydroxide ( $\text{NH}_4\text{OH}$ , ~20%, OCI Co., Korea) and stirred for less than 24 h in an ice bath.<sup>30</sup>

#### **Fabrication of MIM structures**

To measure the electrical characteristics of the  $\text{AlO}_x$  gate dielectric films, MIM structures consisting of Au/ $\text{AlO}_x$ /indium-tin-oxide (ITO) layers were fabricated under various conditions. The  $\text{AlO}_x$  precursor solutions were deposited on ITO-coated glass substrates using a spin-coating



method. Prior to deposition, the ITO-coated glass substrates were consecutively cleaned by ultrasonication in a detergent solution, acetone, and hot isopropyl alcohol. The ITO-coated glass substrates were then dried and treated with ozone plasma for 20 min. The  $\text{AlO}_x$  precursor solutions were spin-coated at 4000 rpm for 30 s and prebaked on a hot plate at 130 °C for 10 min to remove the residual solvent. After prebaking, the  $\text{AlO}_x$  films were annealed at 250 °C for 1 h in a vacuum oven. The circular electrodes (100 nm thickness, Au) were thermally evaporated through a patterned metal shadow mask. The area of the circular electrode was 25 mm<sup>2</sup>.

### **Fabrication and electrical measurement of ZnO TFTs**

A bottom-gate top-contact design was used as a typical device structure for the ZnO TFTs.  $\text{AlO}_x$  precursor solutions were spin-coated and annealed on ITO in the same manner described above to form a gate dielectric layer. The ZnO precursor solutions were then deposited on the obtained  $\text{AlO}_x$  gate dielectric using a spin-coating method. Prior to deposition, the  $\text{AlO}_x$  gate dielectric was treated with ozone plasma for 20 min. The ZnO precursor solutions were spin-coated at 1000 rpm for 45 s and prebaked on a hot plate at 90 °C for 5 min to remove any residual solvents. After pre-baking, the ZnO thin films were annealed at 250 °C for 1 h on a hot plate in ambient air. The top contact source and drain electrodes (120 nm thickness, Al) were thermally evaporated through a patterned metal shadow mask. The ratio of the channel width to length was 60 (width: 3000 μm; length: 50 μm).

The electrical characteristics of the ZnO TFTs were measured in air using an Agilent semiconductor parameter analyzer 4155C. The measurements were typically performed using a continuous method, and the transfer curve was recorded before the output curve. The field-effect

mobility ( $\mu_{\text{lin}}$ ) and the threshold voltage ( $V_{\text{th}}$ ) were calculated for the linear region using Equation 1,

$$I_D = \frac{W}{L} \mu_{\text{lin}} C_i (V_G - V_{\text{th}}) V_{\text{ds}} \quad (1)$$

where  $I_D$  is the saturation current,  $C_i$  is the capacitance per unit area of the dielectric,  $V_G$  is the source-gate voltage, and  $W$  and  $L$  are the TFT channel width and length, respectively.

### Acknowledgments

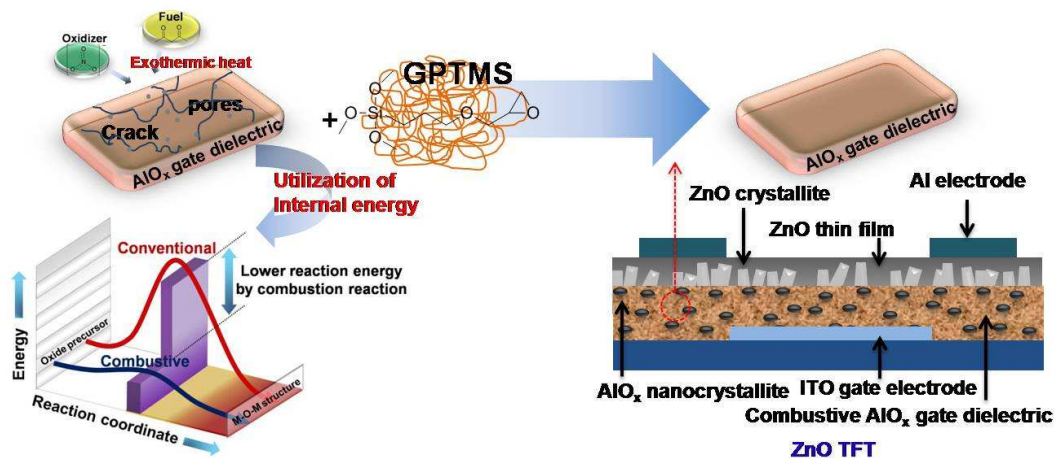
This work was supported by a grant from R&D Convergence Program of Ministry of Science, ICT, and Future Planning and Korea Research Council for Industrial Science and Technology of Republic of Korea (Grant B551179-09-06-00).

### References

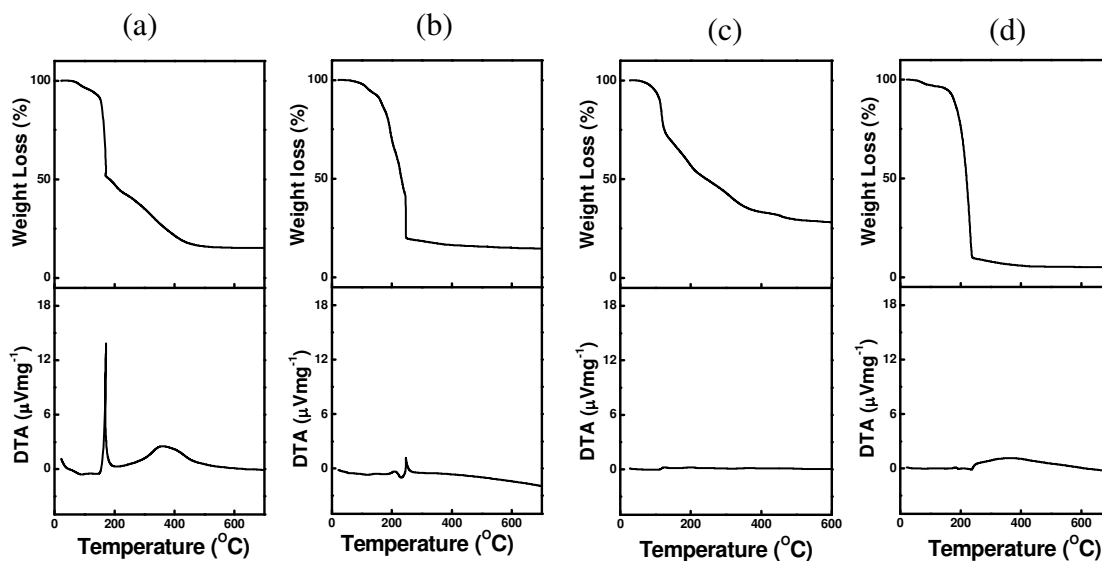
- 1 D. Panda, T. Y. Tseng, *Thin Solid Films*, 2013, **531**, 1-20.
- 2 Y. C. Chang, W. H. Chang, Y. H. Chang, J. Kwo, Y. S. Lin, S. H. Hsu, J. M. Hong, C. C. Tsai, Hong, *Microelectron. Eng.*, 2010, **87**, 2042-2045.
- 3 S. H. Chae, W. J. Yu, J. J. Bae, D. L. Duong, D. Perello, H. Y. Jeong, Q. H. Ta, T. H. Ly, Q. A. Vu, M. H. Yun, X. Duan, Y. H. Lee, *Nat. Mat.*, 2013, **12**, 403-409.
- 4 H. J. Bong, W. H. Lee, D. Y. Lee, B. J. Kim, J. H. Cho, K. W. Cho, *Appl. Phys. Lett.*, 2010, **96**, 192115.

- 5 K. Jiang, J. T. Anderson, K. Hoshino, D. Li, J. F. Wager, D. A. Keszler, *Chem. Mater.*, 2011, **23**, 945-952.
- 6 B. S. Ong, C. Li, Y. Li, Y. Wu, R. Loutfy, *J. Am. Chem. Soc.*, 2007, **129**, 2750-2751.
- 7 W. S. Yang, K. K. Song, Y. H. Jung, S. H. Jeong, J. H. Moon, *J. Mater. Chem. C*, 2013, **1**, 4275-4282.
- 8 J. H. Park, Y. B. Yoo, K. H. Lee, W. J. Jang, J. Y. Oh, S. S. Chae, H. W. Lee, S. W. Han, H. K. Baik, *ACS Appl. Mater. Interfaces*, 2013, **5**, 8067-8075.
- 9 Y. M. Park, D. Jurgen, H. Martin, S. Alberto, *Adv. Mater.*, 2011, **23**, 971-974.
- 10 Y. B. Yoo, J. H. Park, K. H. Lee, H. W. Lee, K. M. Song, S. J. Lee, H. K. Baik, *J. Mater. Chem. C*, 2013, **1**, 1651-1658.
- 11 Y. G. Ha, J. D. Emery, M. J. Bedzyk, H. Usta, A. Facchetti, T. J. Marks, *J. Am. Chem. Soc.*, 2011, **133**, 10239-10250.
- 12 S. T. Meyers, J. T. Anderson, D. Hong, C. M. Hung, J. F. Wager, D. A. Keszler, *Chem. Mater.*, 2007, **19**, 4023-4029.
- 13 S. H. Jeong, S. H. Lee, D. J. Kim, H. J. Shin, J. H. Moon, *J. Phys. Chem. C*, 2007, **111**, 16084-16087.
- 14 K. K. Song, Y. M. Jeong, T. H. Jun, C. Y. Koo, D. J. Kim, K. H. Woo, A. R. Kim, J. H. Noh, S. W. Cho, J. H. Moon, *Jpn. J. Appl. Phys.* 2010, **49**, 05EB02.
- 15 A. C. Geiculescu, T. F. Strange, *Thin Solid Films*, 2006, **503**, 45-54.
- 16 B. N. Pal, B. M. Dhar, K. C. See, H. E. Katz, *Nat. Mat.*, 2009, **8**, 898-903.
- 17 C. Avis, J. Jang, *J. Mater. Chem.*, 2011, **21**, 10649-10652.
- 18 S. S. Manoharan, K. C. Patil, *J. Sol. Sta. Chem.*, 1993, **102**, 267-276.
- 19 H. C. Yi, J. J. Moore, *J. Mater. Sci.*, 1990, **25**, 1159-1168.

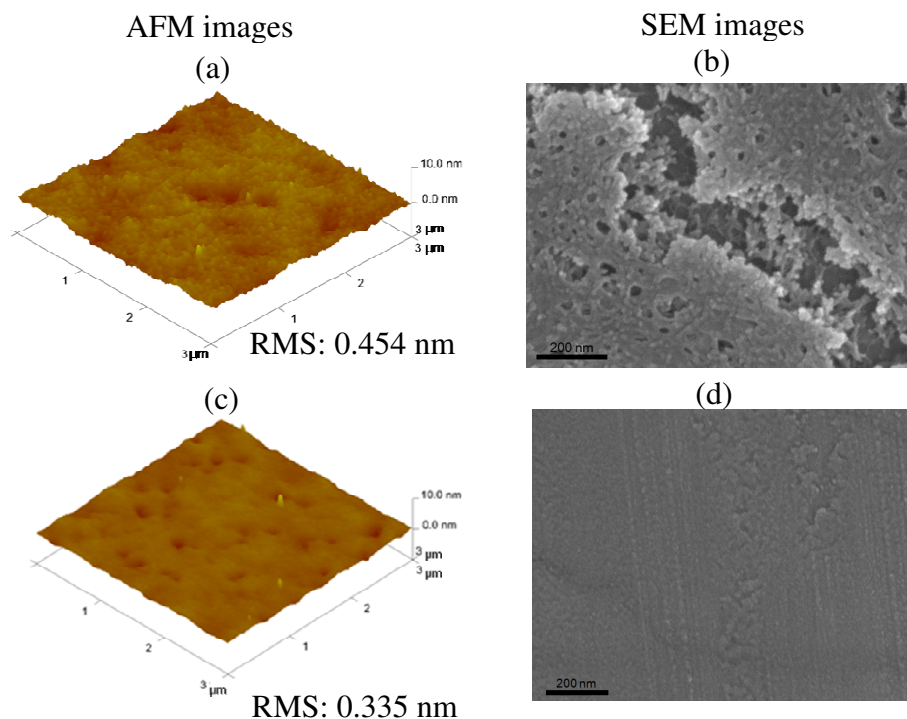
- 20 M. G. Kim, M. G. Kanatzidis, A. Facchetti, T. J. Marks, *Nat. Mat.*, 2011, **20**, 382-388.
- 21 Y. H. Kang, S. H. Jeong, J. M. Ko, J. Y. Lee, Y. M. Choi, C. J. Lee, S. Y. Cho, *J. Mater. Chem. C*, 2014, DOI: 10.1039/C4TC00139G.
- 22 H. J. Ha, S. W. Jeong, T. Y. Oh, M. Kim, K. Choi, J. H. Park, B. K. Ju, *J. Phys. D: Appl. Phys.*, 2013, **46**, 235102.
- 23 C. -C. Hwang, T. -Y. Wu, J. Wan, J. -S. Tsai, *Mater. Sci. Eng. B*, 2004, **111**, 49-56.
- 24 M. Epifan, E. Melissno, G. Pace, M. Schioppa, *J. Euro. Cerm. Soc.*, 2007, **27**, 115-123.
- 25 C. H. Ahn, K. Senthil, H. K. Cho, S. Y. Lee, *Scientific Reports*, 2013, **3**, 2737.
- 26 S. T. Meyers, J. T. Anderson, C. M. Hung, J. Thompson, J. F. Wager, D. A. Keszler, *J. Am. Chem. Soc.*, 2008, **130**, 17603-17609.
- 27 B.S. Ong, C. Li, Y. Li, Y. Wu, R. Loutfy, *J. Am. Chem. Soc.*, 2007, **129**, 2750-2751.
- 28 E. Fortunato, P. Barquinha, A. Pimentel, A. Goncalves, A. Marques, L. Pereira, R. Martins, *Thin Solid Films*, 2005, **487**, 205-211.
- 29 S. V. Lamaka, M. F. Montemor, A. F. Galio, M. L. Zheludkevicha, C. Trindadeb, L. F. Dickb, M. G. S. Ferreiraa, *Electrochimica Acta*, 2008, **53**, 4773-4783.
- 30 S. T. Meyers, J. T. Anderson, C. M. Hung, J. Thompson, J. F. Wager, D. A. Keszler, *J. Am. Chem. Soc.*, 2008, **130**, 17603-17609



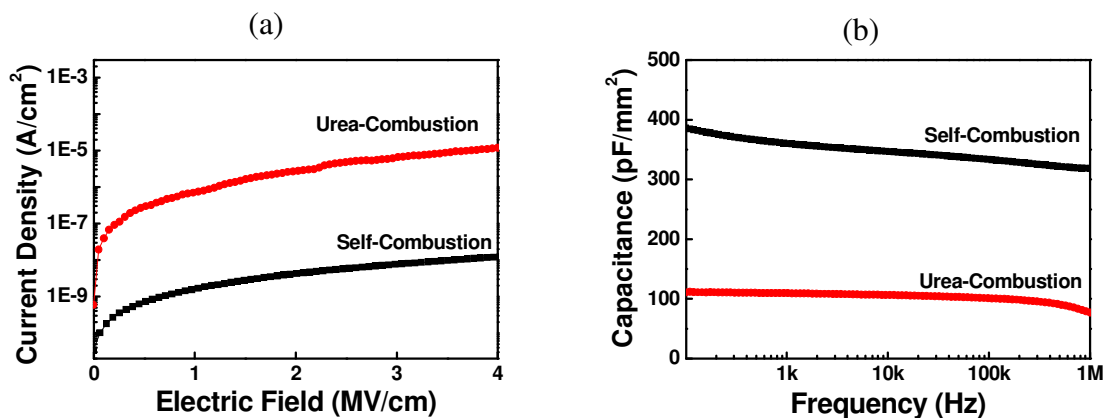
**Scheme 1** Schematic diagram of the  $\text{AlO}_x$  gate dielectric film prepared by self-combustion of metal precursors mixed with organic compounds.



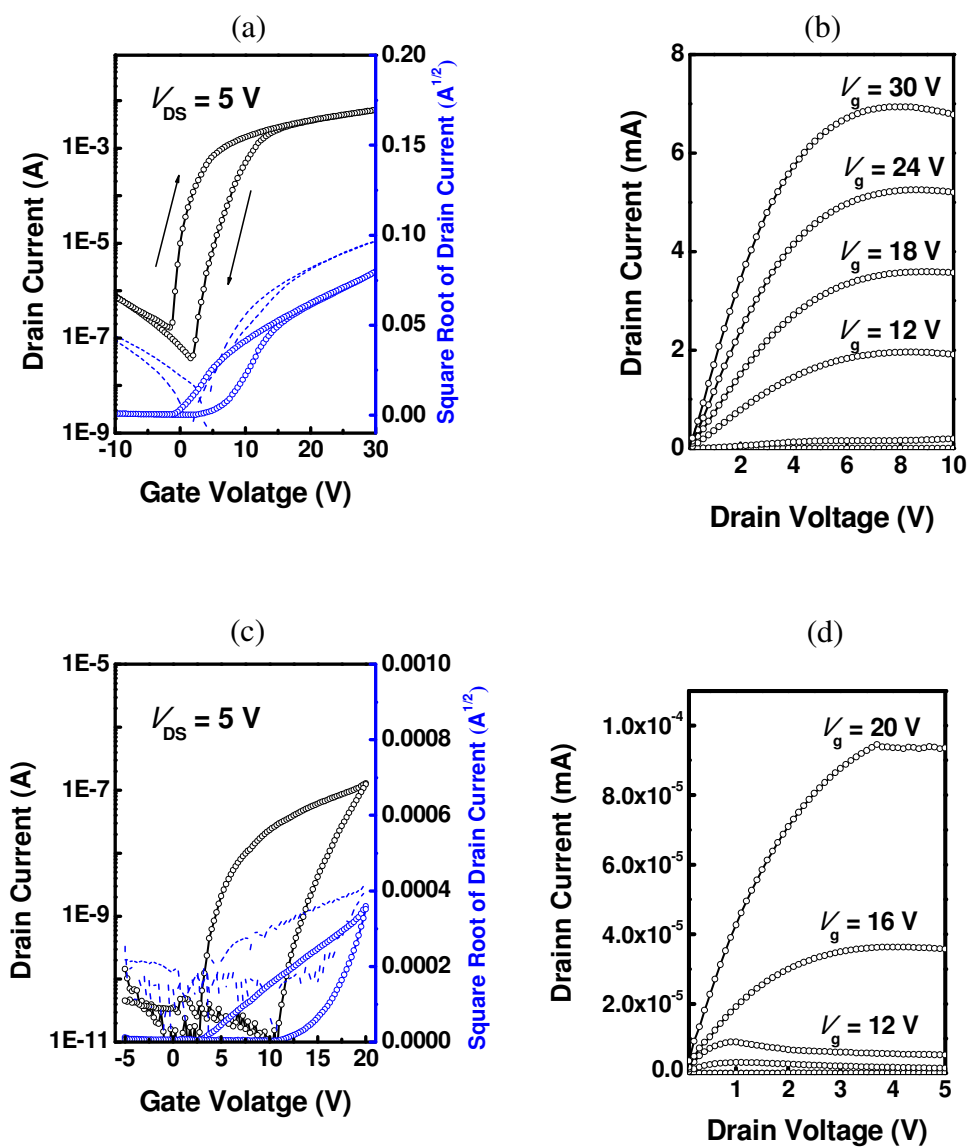
**Fig. 1** TG-DTA curves of combustive and noncombustive precursors: (a) self-combustive  $\text{AlO}_x$  precursor, (b) combustive precursor with urea, (c) noncombustive  $\text{Al}(\text{NO}_3)_3 \cdot 9\text{H}_2\text{O}$ , and (d) noncombustive  $\text{Al}(\text{C}_2\text{H}_5\text{O}_2)_3$ .



**Fig. 2** Atomic force microscope (AFM) step profiler images and surface scanning electron microscope (SEM) images of  $\text{AlO}_x$  thin films prepared by (a, b) self-combustion and (c, d) combustion with urea.



**Fig. 3** (a) Current density vs. electrical field and (b) dependence of capacitance on the frequency for  $\text{AlO}_x$  thin films with GPTMS prepared by self-combustion and combustion with urea.



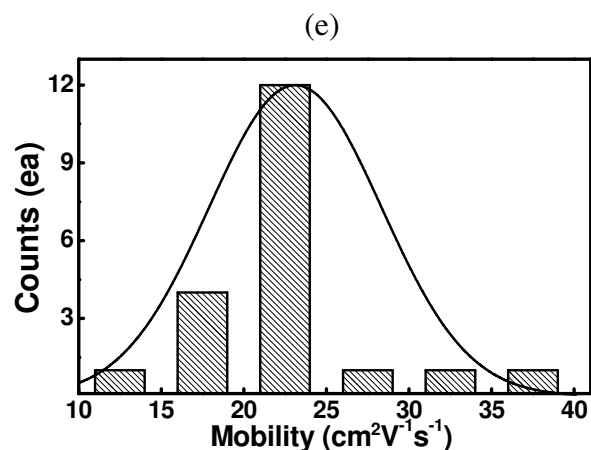


**Fig. 4** (a) Transfer and (b) output characteristics of the ZnO TFTs fabricated from AlO<sub>x</sub> gate dielectrics with 1:8 ratios of the self-combustive AlO<sub>x</sub> precursor to GPTMS. (c) Transfer and (d) output characteristics of the ZnO TFTs fabricated from AlO<sub>x</sub> gate dielectrics with 1:8 ratios of the AlO<sub>x</sub> precursor with urea to GPTMS. (e) Device uniformity of the ZnO TFTs fabricated from AlO<sub>x</sub> gate dielectrics prepared with the self-combustive AlO<sub>x</sub> precursor.



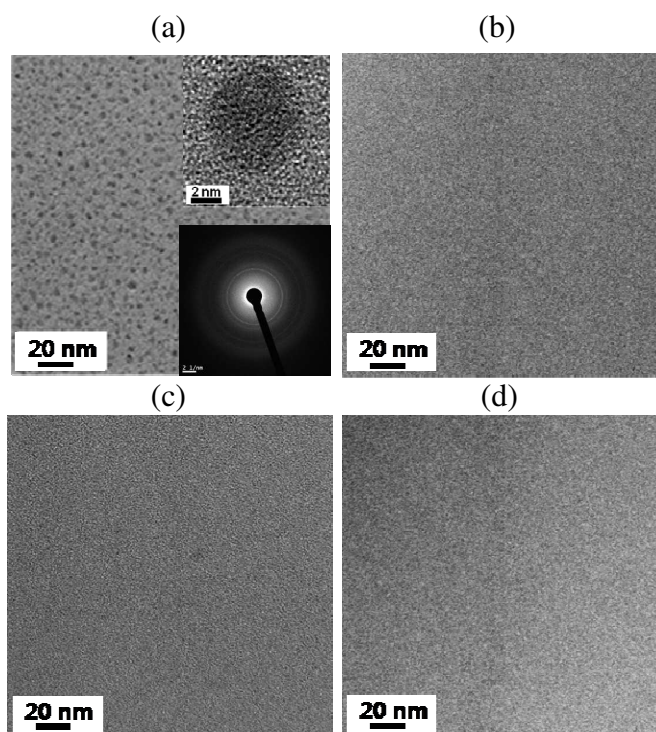


**Fig. 5** TEM images of the  $\text{AlO}_x$  gate dielectric films prepared from the (a) self-combustive  $\text{AlO}_x$  precursor with GPTMS (with insets showing an  $\text{AlO}_x$  nanocrystallite in the film and diffraction pattern), (b) combustive  $\text{AlO}_x$  precursor with urea with GPTMS, (c) noncombustive  $\text{Al}(\text{NO}_3)_3 \cdot 9\text{H}_2\text{O}$  precursor with GPTMS, and (d) noncombustive  $\text{Al}(\text{C}_2\text{H}_5\text{O}_2)_3$   $\text{AlO}_x$  precursor with GPTMS.

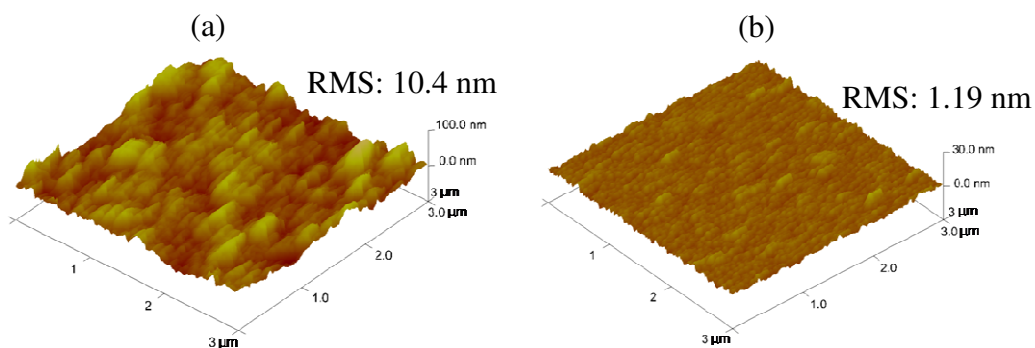


**Fig. 6** AFM images of ZnO films on  $\text{AlO}_x$  thin films (a) without GPTMS and (b) with GPTMS.

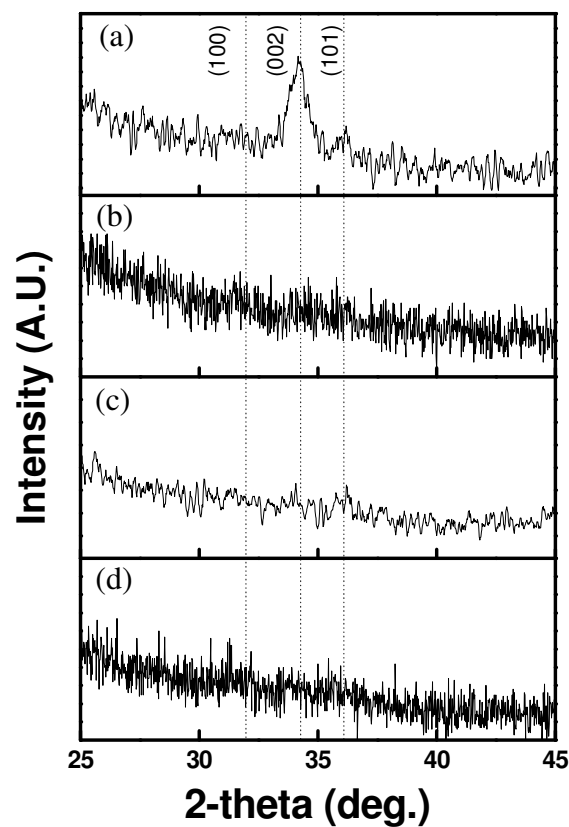


**Fig. 7** XRD patterns of the ZnO thin films on  $\text{AlO}_x$  gate dielectrics prepared from three different precursors after annealing at  $250^\circ\text{C}$ : (a) self-combustive  $\text{AlO}_x$  precursor with GPTMS, (b) combustive  $\text{AlO}_x$  precursor with urea with GPTMS, (c) noncombustive  $\text{Al}(\text{NO}_3)_3 \cdot 9\text{H}_2\text{O}$  with GPTMS, and (d) noncombustive  $\text{Al}(\text{C}_2\text{H}_5\text{O}_2)_3$  with GPTMS.

**Table 1** Electrical properties of films obtained from combustive  $\text{AlO}_x$  precursors mixed with various amounts of GPTMS

| combustive precursor | molar ratio ( $\text{AlO}_x$ Precursor: GPTMS) | dielectric constant (@ 100 Hz) | capacitance ( $\text{pF mm}^{-2}$ ) (@ 100 Hz) | capacitance <sup>a</sup> ( $\text{pF mm}^{-2}$ ) (@ 1 Hz) | leakage current density ( $\text{A cm}^{-2}$ ) (@ 2 MV/cm) | thickness (nm) |
|----------------------|--|--------------------------------|--|---|--|----------------|
|                      | 0:1  | 16.0                           | 700  | -   | -  | 200            |
|                      | 1:8  | 8.7                            | 384  | 426   | $3.29 \times 10^{-9}$                                      | 200            |
| self-combustive      | 1:30   | 10.9                           | 474  | 752   | $6.20 \times 10^{-9}$                                      | 200            |
|                      | 1:45   | 12.0                           | 530  | 868   | $1.40 \times 10^{-8}$                                      | 200            |
|                      | 1:0  |                                |  | N/A   |  |                |
| combustive with urea | 1:8  | 4.4                            | 110  | 110   | $2.80 \times 10^{-6}$                                      | 250            |

<sup>a</sup>Extrapolated to a frequency of 1 Hz

**Table 2** Characteristics of ZnO TFTs fabricated from AlO<sub>x</sub> gate dielectrics with different amounts of GPTMS

| combustive precursor | molar ratio (AlO <sub>x</sub> precursor: GPTMS) | mobility <sup>a</sup> (cm <sup>2</sup> V <sup>-1</sup> s <sup>-1</sup> ) | threshold voltage (V) | on/off ratio |
|----------------------|---|--|-----------------------|--------------|
|                      | 1:0   |  | N/A                   |              |
| self-combustive      | 1:8   | 24.7   | 6.35                  | 1.71E + 05   |
|                      | 1:30  | 13.9   | 8.14                  | 2.35E + 05   |
|                      | 1:45  | 8.97   | 8.32                  | 4.07E + 05   |
| combustive with urea | 1:8   | 2.48 × 10 <sup>-3</sup>  | 7.11                  | 1.00E + 04   |

<sup>a</sup>Calculated from capacitance values extrapolated to a frequency of 1 Hz

The Table of Contents Entry

## Soluble Oxide Gate Dielectrics Prepared Using the Self-Combustion Reaction for High-Performance Thin-Film Transistors

Eun Jin Bae,<sup>a</sup> Young Hun Kang,<sup>a</sup> Mijeong Han,<sup>a</sup> Changjin Lee,<sup>\*a,b</sup> and Song Yun Cho<sup>\*a</sup>

ToC figure.

